

Supporting Information

Toward Organization of Cyano-Bridged Coordination

Polymer Nanoparticles within Ionic Liquid Crystal.

Joulia Larionova,^{†*} Yannick Guari,^{†*} Christophe Blanc,[‡] Philippe Dieudonné,[‡] Alexei Tokarev,[†] and Christian Guérin[†]

[†]*Institut Charles Gerhardt Montpellier and [‡]Laboratoire des Colloïdes, Verres et Nanomatériaux, Université Montpellier II, Place E. Bataillon, 34095 Montpellier, France. Fax : 00(33)467143852. E-mail : joulia.larionova@univ-montp2.fr, yannick.guari@univ-montp2.fr.*

Table S1. Thermal data from DSC and POM observations for [C₁₀-MIM][BF₄] and Mn_{1.5}[Cr(CN)₆]/[C₁₀MIM][BF₄] samples. Enthalpy (J/g) is given within brackets.

Samples	cycle	T _m of water, °C	T _{C-L} , °C (enthalpy, J.G-1)
[C ₁₀ -MIM][BF ₄]	heating	-	2.12 (-49.88)
	cooling	-	-42.05 (18.19)
Mn _{1.5} [Cr(CN) ₆]/[C ₁₀ MIM][BF ₄]	heating	0, Broad	2.67 (-60.24)
	cooling	-	-41.29 (22.4)

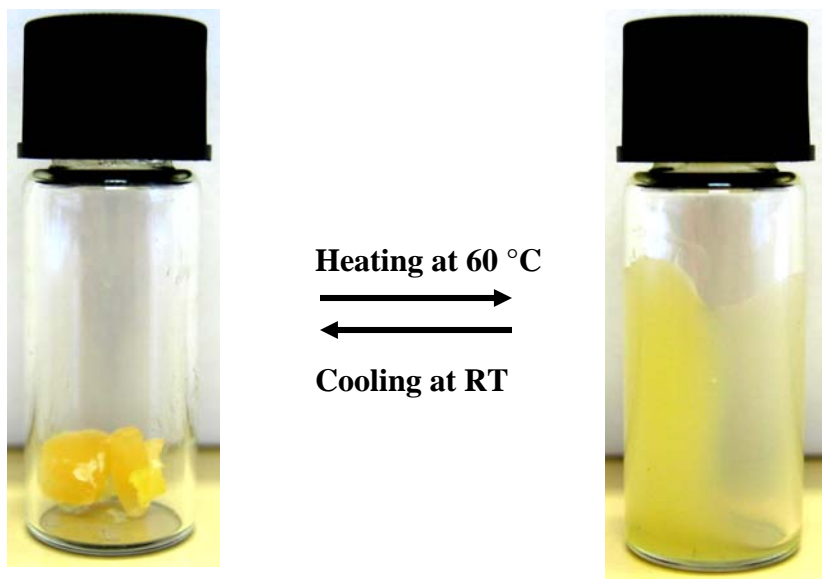


Figure S1. Photograph of the sample $\text{Mn}_{1.5}[\text{Cr}(\text{CN})_6]/[\text{C}_{12}\text{-MIM}] \text{BF}_4$.

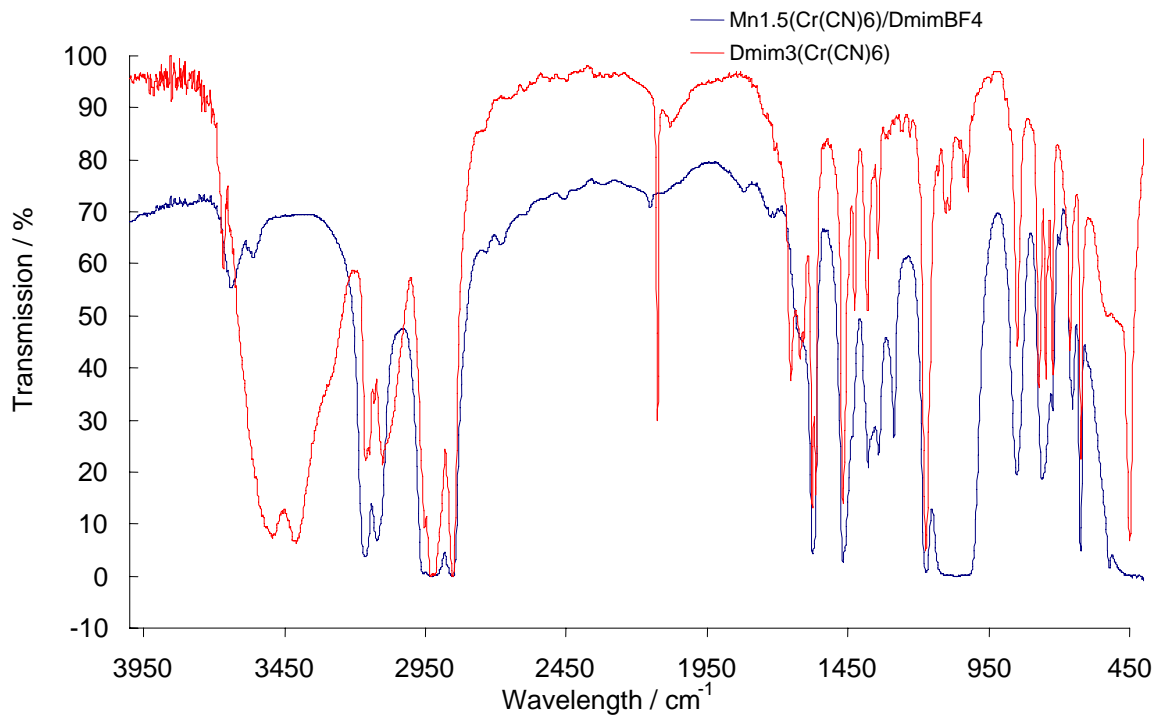


Figure S2. IR spectra of Dmim₃(Cr(CN)₆) and Mn_{1.5}(Cr(CN)₆)/DmimBF₄.

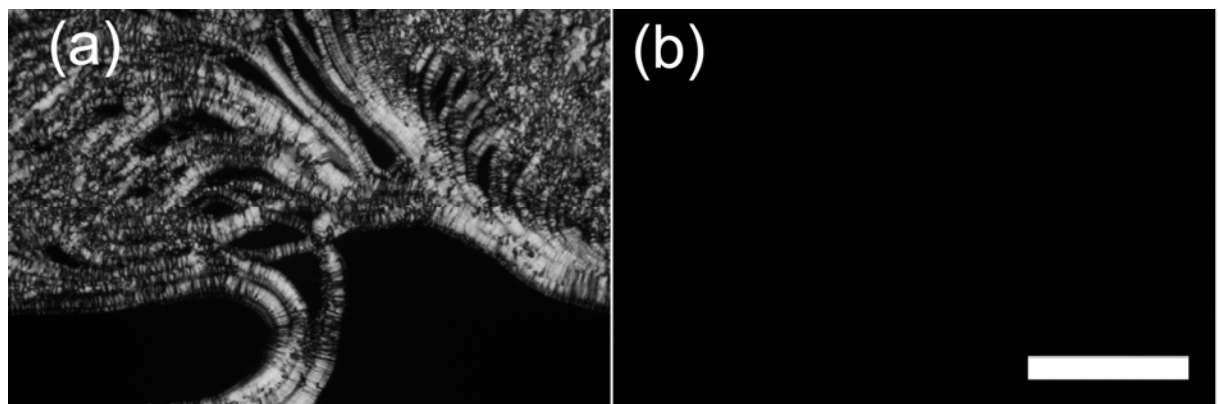


Figure S3. Optical microscopy images under polarized light for the $[C_{12}\text{-MIM}]BF_4$ sample taken at a) $30\text{ }^\circ\text{C}$ and b) $60\text{ }^\circ\text{C}$. Scale bar = $100\text{ }\mu\text{m}$.

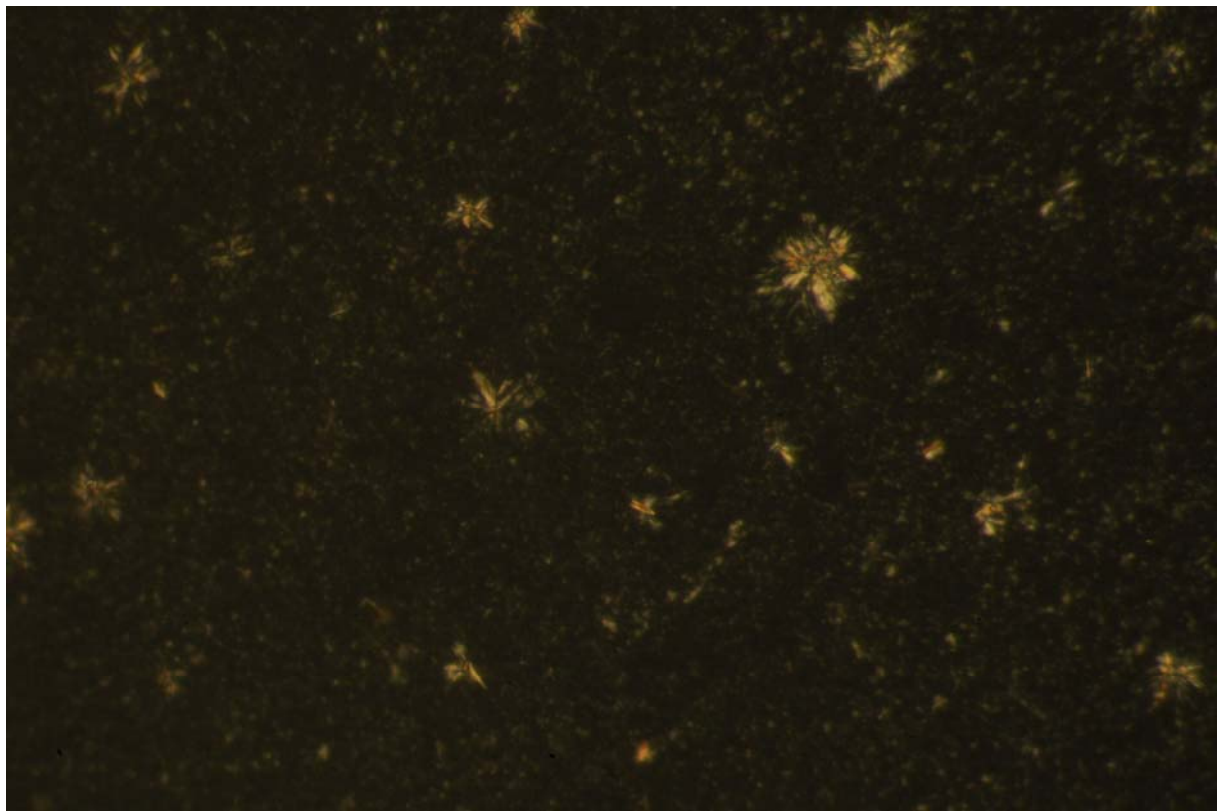


Figure S4. Polarized Optical Microscopy image of the $\text{Mn}_{1.5}[\text{Cr}(\text{CN})_6]/[\text{C}_{12}\text{-MIM}] \text{BF}_4$ sample in the crystalline phase, at 0 °C, with 10 min of waiting showing formation of star-like crystals of water.

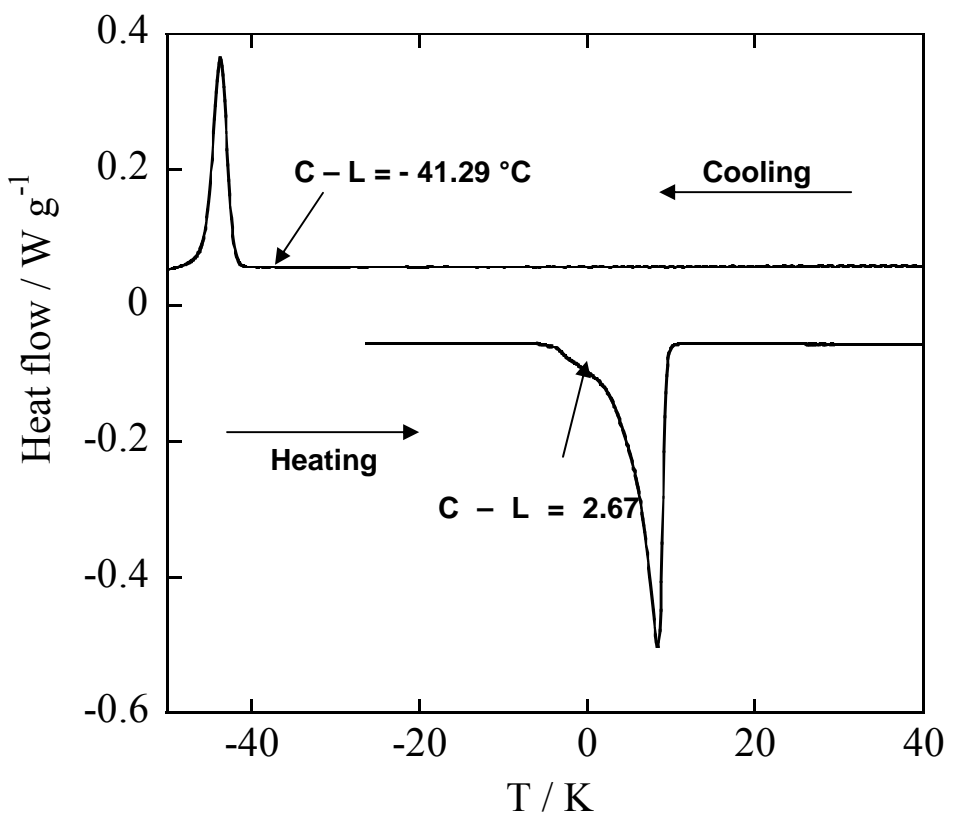
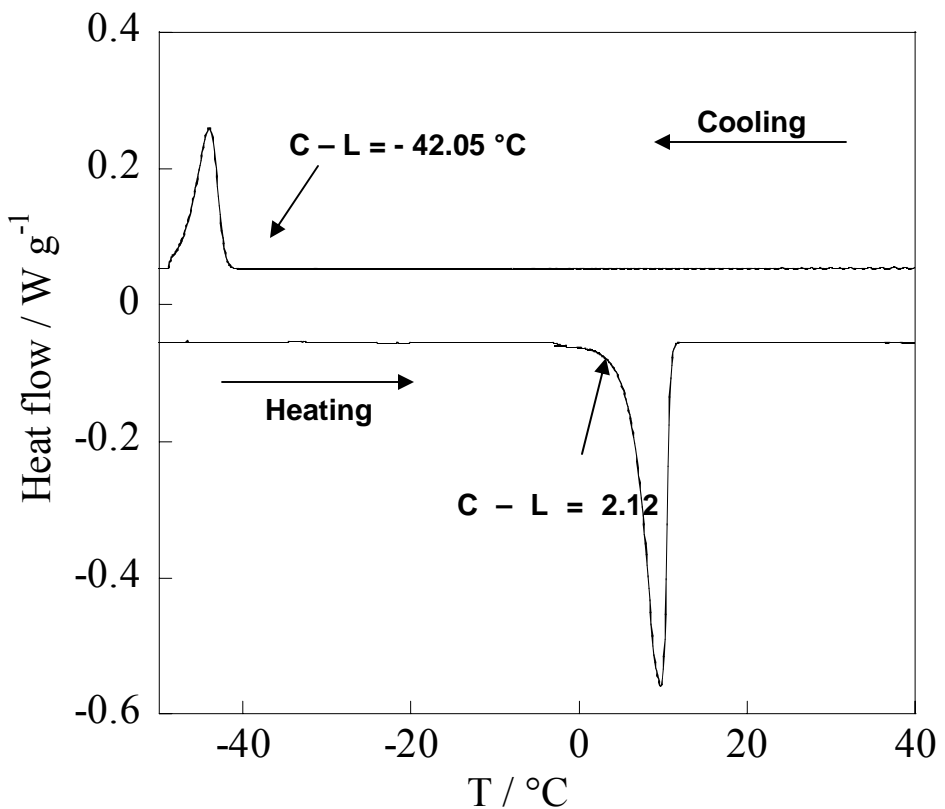


Figure S5. DSC traces of the isotropic ionic liquids a) $[C_{10}\text{-MIM}]BF_4$ for the second heating (lower) and cooling (upper) cycles showing Crystal-Isotropic liquid (C-L) transitions and b) $Mn_{1.5}[\text{Cr}(\text{CN})_6]/[C_{10}\text{-MIM}]BF_4$ sample for the second heating (lower) and cooling (upper) cycles showing Crystal-Isotropic liquid (C-L) transitions.

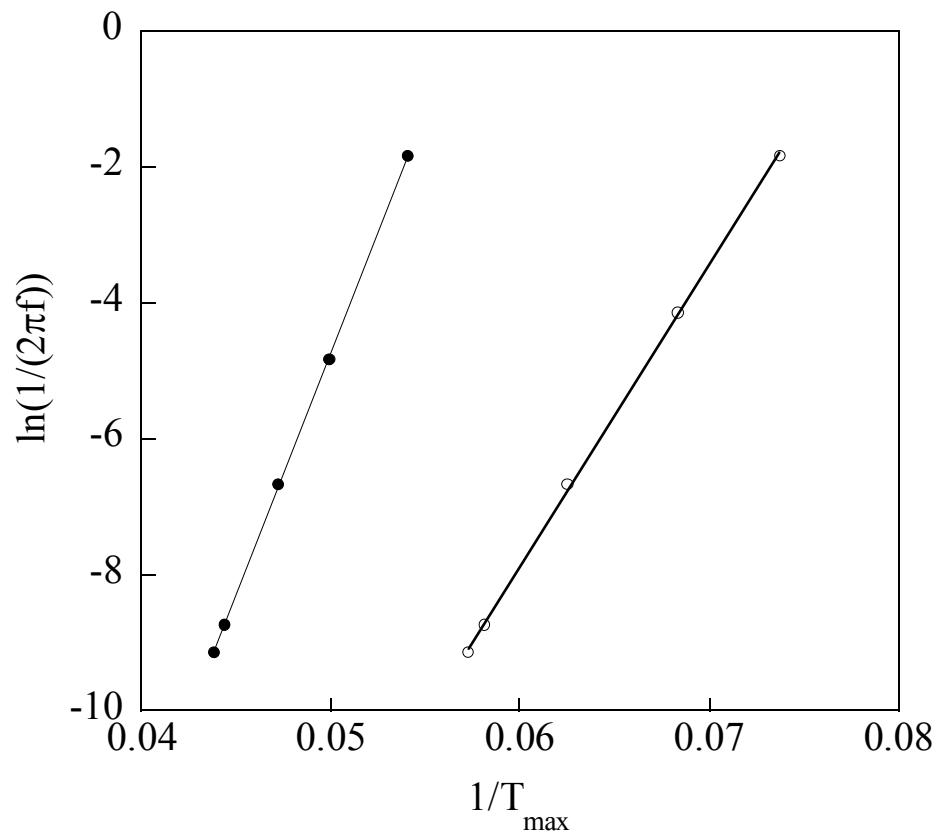
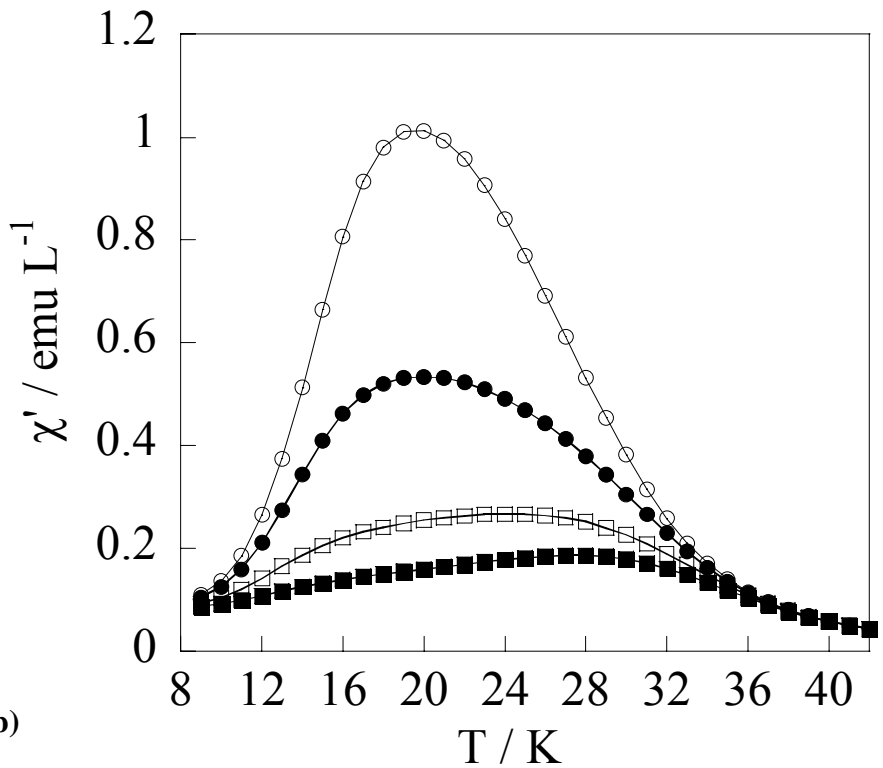


Figure S6. Thermal variation of the relaxation time according to the Arrhenius law for $\text{Mn}_{1.5}[\text{Cr}(\text{CN})_6]/[\text{C}_{12}\text{-MIM}] \text{BF}_4$ (●) and $\text{Mn}_{1.5}[\text{Cr}(\text{CN})_6]/[\text{C}_{10}\text{-MIM}] \text{BF}_4$ (○) samples.

a)



b)

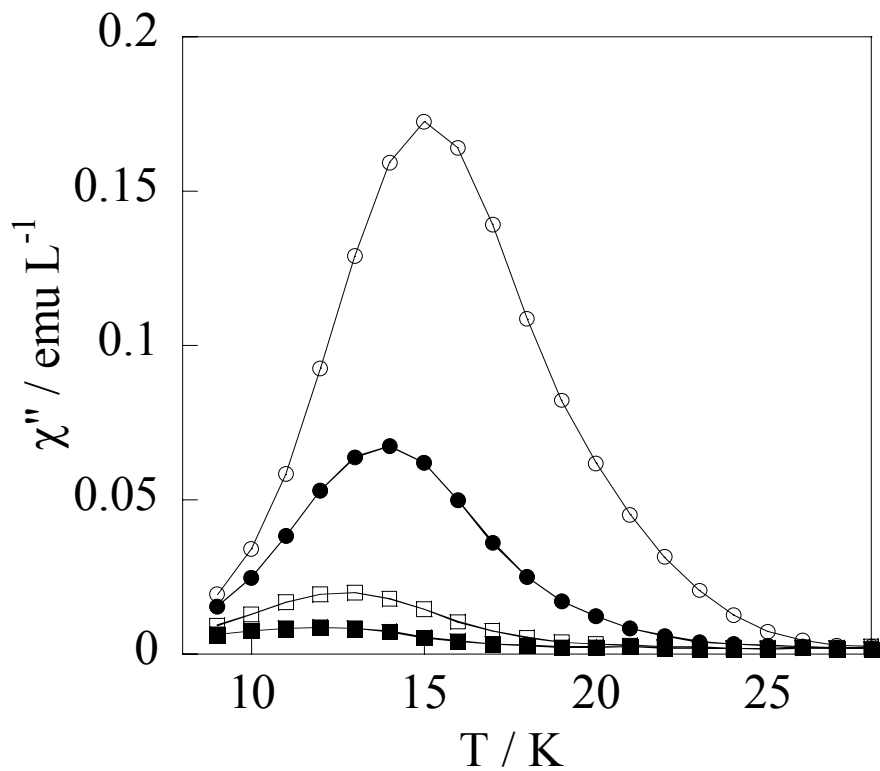


Figure S7. Temperature variation of the a) real and b) imaginary parts of the ac susceptibility performed with different applied fields for $\text{Mn}_{1.5}[\text{Cr}(\text{CN})_6]/[\text{C}_{12}\text{-MIM}] \text{BF}_4$ sample. Applied field: 100 Oe (o); 250 Oe (●), 500 Oe (□) and 750 Oe (■).

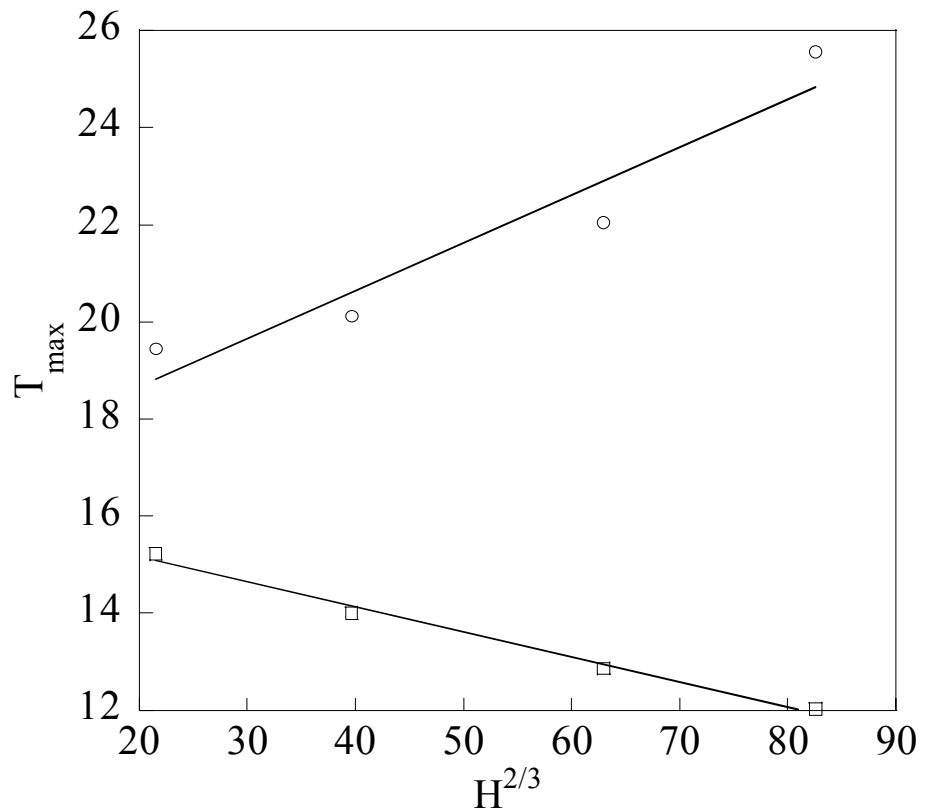


Figure S8. $T_{\max} (\chi')$ and $T_{\max} (\chi'')$ are plotted against $H^{2/3}$ for the $\text{Mn}_{1.5}[\text{Cr}(\text{CN})_6]/[\text{C}_{10}-\text{MIM}] \text{BF}_4$ sample. The solid lines show a linear fit to the data.